

Neural synchrony indexes disordered perception and cognition in schizophrenia

Kevin M. Spencer, Paul G. Nestor, Ruth Perlmutter, Margaret A. Niznikiewicz, Meredith C. Klump, Melissa Frumin, Martha E. Shenton, and Robert W. McCarley*

Department of Psychiatry, Veterans Affairs Boston Healthcare System, Harvard Medical School, Psychiatry 116A, 940 Belmont Street, Brockton, MA 02301

Edited by Rodolfo R. Llinas, New York University Medical Center, New York, NY, and approved October 8, 2004 (received for review August 17, 2004)

Current views of schizophrenia suggest that it results from abnormalities in neural circuitry, but empirical evidence in the millisecond range of neural activity has been difficult to obtain. In pursuit of relevant evidence, we previously demonstrated that schizophrenia is associated with abnormal patterns of stimulus-evoked phase-locking of the electroencephalogram in the γ band (30–100 Hz). These patterns may reflect impairments in neural assemblies, which have been proposed to use γ -band oscillations as a mechanism for synchronization. Here, we report the unique finding that, in both healthy controls and schizophrenia patients, visual Gestalt stimuli elicit a γ -band oscillation that is phase-locked to reaction time and hence may reflect processes leading to conscious perception of the stimuli. However, the frequency of this oscillation is lower in schizophrenics than in healthy individuals. This finding suggests that, although synchronization must occur for perception of the Gestalt, it occurs at a lower frequency because of a reduced capability of neural networks to support high-frequency synchronization in the brain of schizophrenics. Furthermore, the degree of phase locking of this oscillation is correlated with visual hallucinations, thought disorder, and disorganization in the schizophrenia patients. These data provide support for linking dysfunctional neural circuitry and the core symptoms of schizophrenia.

electroencephalogram | γ band

Contemporary views of schizophrenia propose that the basis of this disorder lies in the dysfunction of neural microcircuits, rather than specific brain areas or neurotransmitter systems. These views are based on postmortem studies of the brains of schizophrenia patients (SZ), which have reported abnormalities at the cellular level, including inhibitory interneurons (1–3). Moreover, animal studies suggest that such disturbances may involve the hypofunctioning of *N*-methyl-D-aspartate receptors on inhibitory interneurons because psychotomimetics selectively block this receptor (4, 5). Inhibitory interneurons appear to be crucial elements in the generation of synchronous neural activity in the β (13–30 Hz) and γ (30–100 Hz) bands of the electroencephalogram (EEG) (6, 7). Evidence is accumulating that such synchronous oscillations may underlie cognitive functions such as object perception, selective attention, and working memory (8, 9), as well as consciousness (10). Thus, the analysis of high-frequency EEG oscillatory activity may provide functional evidence for neural circuitry abnormalities in schizophrenia.

In earlier studies we have found that SZ exhibit deficits in γ -band neural synchrony as measured by EEG phase locking during auditory steady-state stimulation (11) and during the perception of visual Gestalt patterns (12). In the latter study, SZ displayed several abnormalities in the early visual γ -band oscillation in comparison with matched healthy control subjects. The most striking finding was that Gestalt stimuli failed to elicit the occipital component of the early γ -band oscillation in schizophrenics, suggesting that their visual feature-binding processes were abnormal. However, there was no relationship between this effect and symptomatology.

We hypothesized that a clearer relationship between neural synchrony and schizophrenic symptoms might be found if we

examined oscillations that were phase-locked to reaction time (RT), rather than stimulus onset. Because single-unit recording studies have found that the processes associated with making a perceptual decision are more correlated with RT than stimulus onset time (13), response-locked oscillations might be more closely related to the feature-binding processes that support conscious perception than stimulus-locked oscillations. Furthermore, a series of psychophysical studies by Silverstein and coworkers (14, 15) has found that deficits in visual Gestalt perception are associated with disorganization and thought disorder in chronic schizophrenics and schizotypal individuals. Therefore, schizophrenic abnormalities in a putative response-locked signature of Gestalt perception might be closely related to these core symptoms of schizophrenia.

In the present study, 20 chronic SZ and 20 normal control subjects (NC) performed the same Gestalt perception task as in our previous report (12). Phase locking (9, 16) was used as a measure of neural synchrony at the macroscopic level of the scalp-recorded EEG and was computed separately on stimulus- and response-locked single trials.

Methods

Subjects. Inclusion criteria for all subjects were: (i) 18–55 years of age; (ii) right-handedness; (iii) no history of electroconvulsive treatment; (iv) no history of neurological illness; (v) no history of alcohol or drug dependence or abuse within the last year, or long duration (>1 year) of past abuse; (vi) no present medication for medical disorders that would have deleterious EEG, neurological, and/or cognitive consequences; (vii) verbal IQ of >75; (viii) no alcohol use <24 h before testing; and (ix) an ability and desire to cooperate with our experimental procedures as evinced by giving informed consent (following Veterans Affairs Boston Healthcare System and Harvard Medical School guidelines).

Participants in this study were 23 SZ, diagnosed according to the DSM-IV Diagnostic Criteria (17), and 21 NC (all male). Three of the patients' data were unusable, one because of artifacts, the others because of excessive error rates (> 20% in at least one condition). The final SZ sample consisted of 20 [age, 41.8 ± 9.2 years; age at onset, 22.5 ± 4.9 ; total positive symptom score on the Positive and Negative Syndrome Scale (18), 18.1 ± 8.8 ; total negative symptom score, 21.2 ± 7.3]. Two SZ were receiving conventional neuroleptics, 16 SZ were receiving atypical antipsychotics, and 2 SZ received both types. Mean equivalent chlorpromazine dosage was 412 ± 312 mg per day (range of 67–1,200).

Of the NC, one subject's data were unusable because of artifacts, leaving a final sample of 20 (age, 43.1 ± 6.4 years). The SZ and NC groups did not differ on the basis of age ($P = 0.59$)

This paper was submitted directly (Track II) to the PNAS office.

Abbreviations: EEG, electroencephalogram; RT, reaction time; SZ, schizophrenia patient(s); NC, normal control subject(s); VEP, visual evoked potential; VH, visual hallucinations; NVH, non-VH.

*To whom correspondence should be addressed. E-mail: robert.mccarley@hms.harvard.edu.

© 2004 by The National Academy of Sciences of the USA

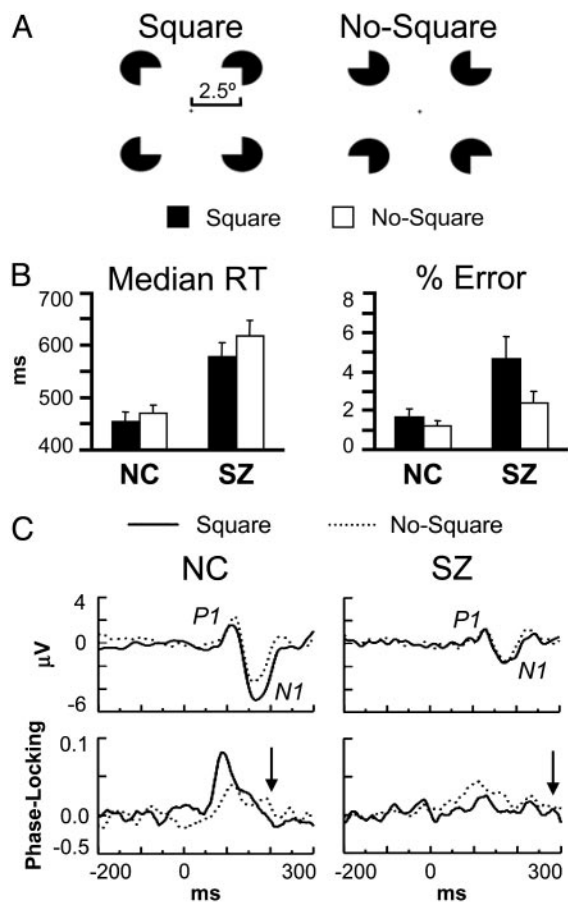


Fig. 1. Gestalt perception task. (A) Stimuli. The ratio of inducer radius to square length is 0.2. (B) RT and error data (bars indicate SE). (C) Grand average VEPs (Upper) and stimulus-locked phase-locking values (Lower; 34.1–40.5 Hz) at electrode O1. Arrows indicate the latency of the response-locked oscillation in the square condition relative to stimulus onset for each group.

or parental socioeconomic status ($P = 0.99$). The stimulus-evoked data from 12 SZ and 12 NC have been reported (12).

Stimuli and Experimental Procedures. Subjects fixated on a central cross and responded with a button press according to whether an illusory square (Fig. 1A) was present or absent. Stimuli remained visible until 300 ms after a response had been made. If no response had been made by 2,000 ms after stimulus onset, the trial was ended and the next trial began (1,000-ms intertrial interval). Subjects performed one practice block and two experimental blocks, each consisting of 45 trials per condition. Response hands were counterbalanced across subjects.

Electrophysiological Recording and Processing. The EEG was recorded (0.01–100 Hz, 500-Hz digitization rate) with tin electrodes at 16 scalp sites (F3/Fz/F4, C3/Cz/C4, P3/Pz/P4, O1/Oz/O2, T5/T6, and PO5/PO6) and the right mastoid, referenced to the left mastoid. The vertical and horizontal electrooculograms were recorded, respectively, at Fp1 and the outer canthi of the eyes. Electrode impedances were <5 k Ω . Error and no-response trials were excluded from analyses. Independent component analysis (19) was used to correct for eyeblink artifacts. Corrected single-trial epochs were re-referenced to averaged mastoids. The SZ and NC groups had averages of 84.9 and 86.6 trials per condition, respectively.

Time-Frequency Analysis. For the response-locked analyses, each single-trial epoch was shifted according to the RT on that trial.

The Morlet wavelet transform (9) was applied to the 20- to 100-Hz frequency range of the EEG on correct-response trials for stimulus- and response-locked epochs. Wavelet center frequencies were 20.3, 22.1, 24.1, 26.3, 28.7, 31.3, 34.1, 37.2, 40.5, 44.2, 48.2, 52.6, 57.3, 62.5, 68.2, 74.3, 81.1, 88.4, and 96.4 Hz. Phase locking was computed as 1 minus the circular variance of phases at each time point, wavelet frequency, and electrode (9, 16). Baseline levels were subtracted from each time-frequency map (stimulus-locked, -200 to -50 ms relative to stimulus onset; response-locked, -50 to $+50$ ms relative to RT).

Dependent variables were analyzed by using ANOVA with the factors group (NC/SZ), stimulus (Square/No-Square), and the appropriate factors for electrode site. For within-subjects factors with more than two levels, the Greenhouse–Geisser correction for inhomogeneity of covariance (20) was used and is reflected in the reported P values. Pearson's r was used for correlation analyses (two-tailed; $n = 20$ unless noted).

Results

Task Performance. SZ made more errors [$F(1,38) = 6.22, P < 0.05$] and had longer median RTs [$F(1,38) = 16.9, P < 0.0001$] than NC (Fig. 1B). SZ also made more errors in response to Square than No-Square stimuli [$F(1,19) = 5.56, P < 0.05$]. Both groups had shorter RTs in response to Square than No-Square stimuli [NC, $F(1,19) = 6.46, P < 0.05$; SZ, $F(1,19) = 18.3, P < 0.001$], with this effect being larger for SZ [group \times stimulus, $F(1,38) = 4.84, P < 0.05$].

Visual Evoked Potentials (VEPs). The average amplitude of the P1 and N1 (Fig. 1C) was measured at occipital (O1/O2), temporal (T5/T6), and parietooccipital (PO5/PO6) electrodes (P1, 90–130 ms NC, 110–140 ms SZ; N1, 130–206 ms NC, 140–212 ms SZ). The P1 was smaller for SZ than NC at right hemisphere sites in the Square condition [$F(1,38) = 6.94, P < 0.05$; group \times stimulus \times hemisphere, $F(1,38) = 9.12, P < 0.01$]. The N1 was smaller overall in SZ than NC [$F(1,38) = 5.37, P < 0.05$] and tended to be larger for Square than No-Square stimuli in both groups [NC, $F(1,19) = 13.6, P < 0.01$; SZ, $F(1,19) = 4.29, P = 0.052$].

Stimulus-Locked Oscillations. For NC (Fig. 2 Upper), Square stimuli elicited the early visual γ -band oscillation at occipital electrodes (O1/Oz/O2, 72–98 ms, 34.1–40.5 Hz). This oscillation was absent in the No-Square condition [$F(1,19) = 8.96, P < 0.01$]. The Square minus No-Square effect was largest at the left occipital site O1 [$t(19) = 3.38, P < 0.01$]. A similar effect of Gestalt perception on early γ -band phase locking has been reported by Rodriguez *et al.* (16), although at a longer latency. For SZ (Fig. 2 Lower), neither stimulus elicited this oscillation [$F(1,19) = 0.602, P = 0.45$; group \times stimulus, $F(1,38) = 6.90, P < 0.05$]. These data confirm the findings of our previous study (12) with a larger sample.

A second effect was present at parietal sites (P3/Pz/P4) for NC: phase locking was enhanced for Square compared to No-Square stimuli in the 136- to 188-ms, 28.7- to 34.1-Hz range [$F(1,19) = 9.95, P < 0.01$]. This effect was most significant at the left parietal electrode P3 [$t(19) = 4.53, P < 0.001$; stimulus \times site, $F(2,38) = 11.8, P < 0.001$]. [There was some overlap in time and frequency between the parietal effect and the N1 VEP, but as the parietal effect was not correlated with N1 amplitude ($r = -0.18, P = 0.44$), we conclude that it is another oscillatory response to Square stimuli rather than an artifact of changes in the N1.] For SZ the parietal effect was not present [$F(1,19) = 1.72, P = 0.21$; group \times stimulus, $F(1,19) = 9.53, P < 0.01$].

Response-Locked Oscillations. Oscillations that preceded and were phase-locked to RT were found in the data of both groups (Fig. 3). For NC, Square stimuli elicited an oscillation in the -270 - to -216 -ms, 31.3- to 44.2-Hz range at occipital sites. This oscillation

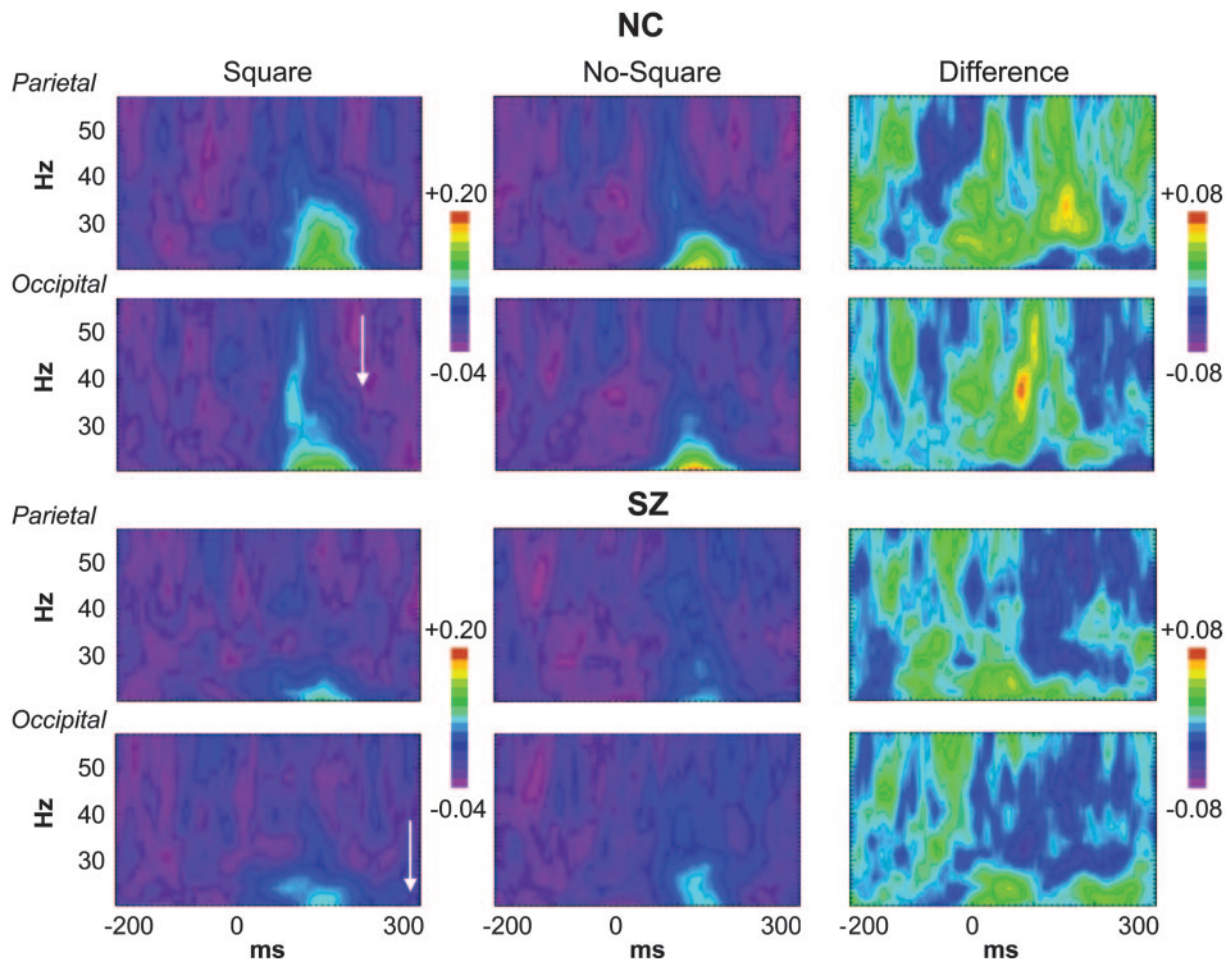


Fig. 2. Grand average stimulus-locked time-frequency maps of phase-locking values for NC and SZ. The left parietal (P3) and occipital (O1) sites are shown. Color scales indicate phase-locking values. The frequency and stimulus-locked latency of the response-locked oscillations are indicated by the arrows.

tion was absent in the No-Square condition [$F(1,19) = 12.6, P < 0.01$]. As with the early occipital stimulus-locked oscillation, this effect was largest at the left occipital site [$t(19) = 3.69, P < 0.01$].

The occipital response-locked oscillation could be the most direct manifestation of visual feature-binding processes yet reported at the macroscopic EEG level and, to our knowledge, has not been previously described. [However, a potential analog in area V2 of the monkey was recently reported (21).] The fact that this oscillation is elicited by Gestalt patterns and is phase-locked to RT suggests that it could reflect the neural mechanisms involved in linking the elements of the illusory square into a coherent percept. Furthermore, its scalp topography is consistent with generators in visual cortex. The similarity between the frequency ranges and topographies of the stimulus- and response-locked occipital oscillations suggests the possibility that the response-locked oscillation reflects the reactivation of the same cell assembly that was initially activated at stimulus presentation. Supporting this hypothesis, we did not find a significant difference between the topographies of the two oscillations [measured across occipital, temporal, and parieto-occipital electrodes; oscillation \times electrode, $F(6,114) = 1.75, P = 0.18$].

For SZ, no oscillations were observed in the same latency and frequency range as for the NC group [$F(1,19) = 0.132, P = 0.72$; group \times stimulus, $F(1,38) = 4.54, P < 0.05$]. However, a response-locked oscillation was elicited by Square stimuli at occipital sites in a lower frequency range (from 22.1 to 24.1 Hz) and at a longer latency before RT (-300 to -266 ms). The

topography of this oscillation was very similar to that in the NC data, again maximal at the left occipital site. Moreover, between-group comparisons of the topographies of the occipital oscillations did not find any significant differences ($P > 0.13$), compatible with the same mechanism operating in both groups.

A second response-locked oscillation was found in the SZ data. At parietal electrodes, Square stimuli evoked a prominent oscillation in the -280 to -216 -ms, 22- to 26-Hz range. This oscillation was not present in the No-Square condition [$F(1,19) = 17.6, P < 0.001$], nor was it elicited by either stimulus for NC [group \times stimulus, $F(1,38) = 4.28, P < 0.05$]. The group effect was maximal at the left parietal site P3 [group \times stimulus \times electrode, $F(2,76) = 4.54, P < 0.05$; group \times stimulus at P3, $F(1,38) = 12.8, P < 0.001$], similar to the stimulus-locked parietal oscillation in NC. The parietal oscillation was distinguished from the occipital oscillation by its shorter latency to RT and wider frequency range. The magnitudes of the parietal and occipital oscillations were not correlated ($r = 0.20, P = 0.39$), confirming that they constituted separate effects.

Clinical Symptom Correlations. We examined correlations between the above phase-locking effects (Square – No-Square) and schizophrenic symptoms on the Positive and Negative Syndrome Scale (18) and Scale for the Assessment of Negative Symptoms (22)/Scale for the Assessment of Positive Symptoms (23). Our focus was on perceptual and cognitive symptoms, particularly hallucinations, attention, delusions, disorganization, and

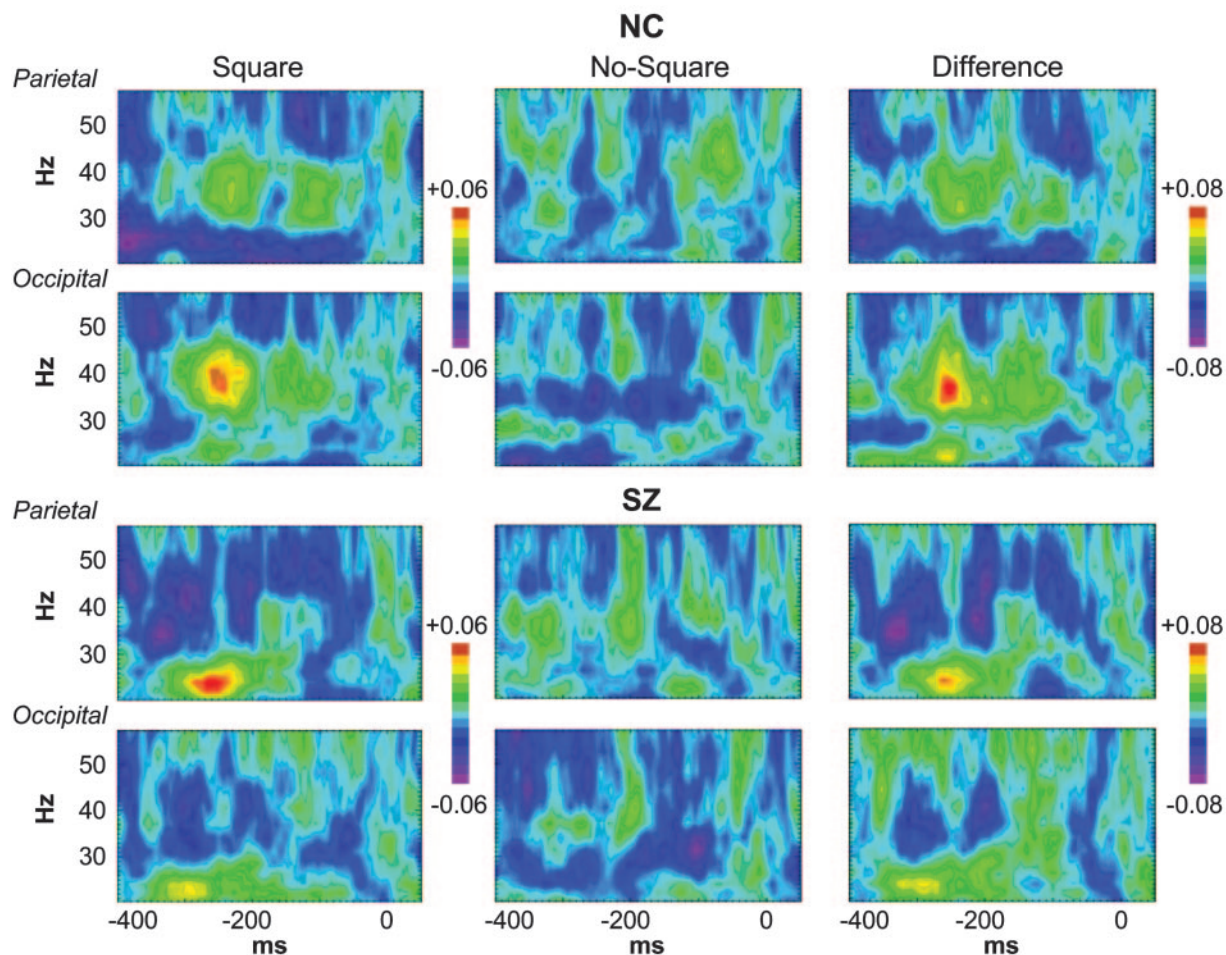


Fig. 3. Grand average response-locked phase-locking maps, as in Fig. 2. The RT on each trial is shifted to 0 ms.

thought disorder. Here, we report only correlations with absolute values >0.5 and P values of <0.01 (see Fig. 4A). These correlations were also significant according to the nonparametric Spearman's ρ .

The occipital response-locked effect was significantly correlated with several positive symptoms: conceptual disorganization ($r = 0.58$) on the Positive and Negative Syndrome Scale (18), and visual hallucinations ($r = 0.56$), thought withdrawal (a delusion subscale) ($r = 0.65$), and the global thought disorder rating ($r = 0.61$) on the Scale for the Assessment of Positive Symptoms (23). In contrast, the parietal response-locked effect was correlated with negative symptoms: the total negative symptom scale on the Positive and Negative Syndrome Scale (18) ($r = 0.57$), and social inattentiveness on the Scale for the Assessment of Negative Symptoms (22) ($r = 0.66$). There was no correlation between medication dosage and these symptoms.

None of the other phase-locking effects correlated significantly with symptoms. Nor was the peak frequency of the occipital response-locked effect, which differed between groups, correlated with any symptom scales. None of the phase-locking effects were correlated with age, age of onset, or medication dosage (all $P > 0.09$).

The pattern of the correlation between the occipital response-locked effect and visual hallucinations suggests that it reflects an overall difference between patients who experienced visual hallucinations [visual hallucinators (VH) ($n = 7$)] and those who did not [nonvisual hallucinators (NVH) ($n = 13$)]. The occipital response-locked effect was significantly greater for VH than

NVH [$t(18) = 2.80$, $P < 0.05$], but when VH were considered alone, the correlation was no longer significant ($r = 0.35$, $P = 0.44$). Because the size of the VH sample was small, the reliability of the group difference was assessed further by using a permutation test in which the VH and NVH patients were assigned at random to groups of 7 and 13, and the t test was computed 1,000 times. Using this method, the significance of the observed group difference was found to be $P < 0.01$.

The VEPs for the VH and NVH were also examined. In the grand averages, with the N1 appears reduced in VH compared with NVH patients (Fig. 4B). This difference was significant in the Square condition at the temporal electrodes [T5/T6, $t(18) = -2.20$, $P < 0.05$; permutation test, $P < 0.05$].

Discussion

The main findings of this study are as follows. (i) A γ -band oscillation is elicited by perceived Gestalt stimuli at occipital electrodes that is phase-locked to RT, making it a potential signature of feature-binding processes in visual cortex. (ii) In individuals with schizophrenia, an oscillation with a similar topography occurs in a lower frequency range than in healthy individuals. (iii) The phase-locking aspect of the SZ oscillation is correlated with core symptoms of schizophrenia. We have demonstrated a link between perceptual and cognitive disturbances, feature-binding processes, and abnormal neural synchrony.

These data suggest that the occipital response-locked oscillation reflects feature-binding processes in both the NC and SZ groups, although further experiments will be necessary for

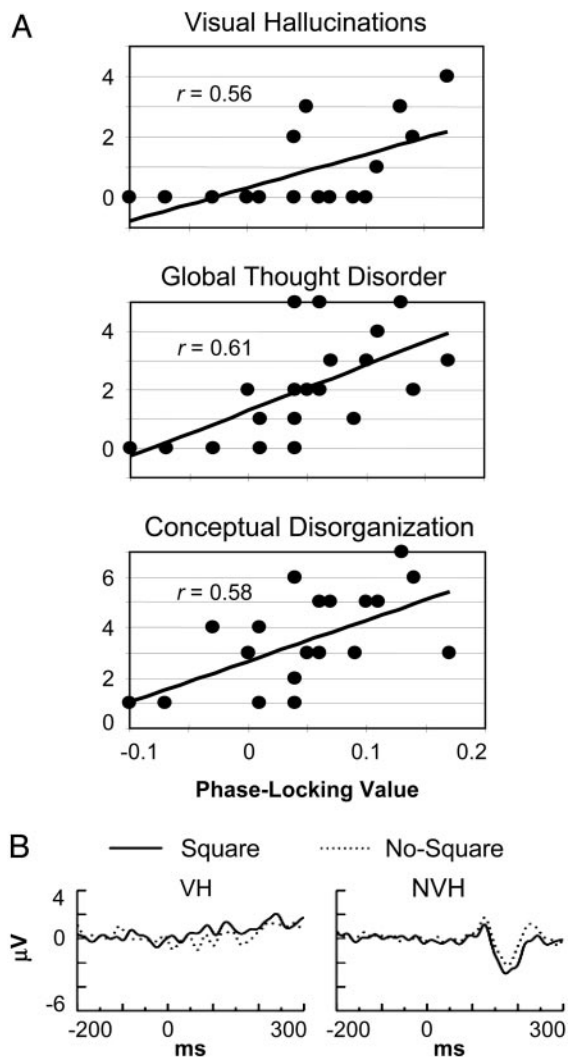


Fig. 4. SZ symptom analyses. (A) Correlations between symptom scales (*y* axis) and the occipital response-locked effect (*x* axis) for SZ. (B) VEPs for the VH and NVH patients at O1.

definitive confirmation. Within the SZ group, the correlations between this oscillation and the conceptual disorganization and thought disorder scales in the patients are consistent with similar correlations reported by Silverstein and coworkers (14, 15) by using psychophysical measures of Gestalt perception. The high degree of convergence between their psychophysical data and the present results supports the proposal of Phillips and Silverstein (24) that thought disorder and disorganization are caused by dysfunctional coordinating interactions in the brains of schizophrenics. A role for the occipital response-locked oscillation in feature-binding processes is further suggested by the relationship between this oscillation and visual hallucinations.

The occipital response-locked oscillation had two abnormalities in the SZ group. First, the frequency of this oscillation was lower than in NC. This finding suggests that a dysfunction rendered the underlying neural circuitry unable to synchronize at a high frequency. One possible cause of this effect could be decreased connectivity, as Kopell *et al.* (25) have demonstrated that synchronization frequency depends on conduction velocity in simulations of neural circuits, and there is abundant evidence for white matter deficits in schizophrenia (26). There is also evidence for reduced excitatory input to pyramidal cells in schizophrenia (2, 27–30), which might also explain the synchro-

nization at a lower frequency. As Steriade *et al.* (31) have shown that more negative values of pyramidal cell membrane potential favor lower frequency oscillations, the reduced synchronization frequency in SZ could be caused by disfacilitation from reduced thalamic inputs (30) and/or a reduction in inhibitory neurotransmission (4, 30).

The second abnormality of the occipital response-locked oscillation (and for the parietal response-locked oscillation) was that increases in symptom ratings were associated with increased, rather than decreased, phase-locking effects. One possibility is that increased phase locking could be related to the phenomenon of cortical hyperexcitability that has been reported in studies of schizophrenia by using transcranial magnetic stimulation (32, 33). It is notable that auditory hallucinations are reduced by the application of slow repetitive transcranial magnetic stimulation, which reduces the excitability of the underlying cortex (34). Furthermore, a neuroimaging study by ffytche *et al.* (35) reported that visual hallucinations were associated with increased baseline activation of visual cortex, which is consistent with increased cortical excitability. This study also reported that the visual cortex of hallucinators was less responsive to external stimulation, which we also found in the lower N1 VEP of the VH subgroup. Still another possibility is that the correlations between increased phase locking and symptoms reflects the presence of abnormally increased connectivity in particular neural circuits, as was recently reported for SZ with auditory hallucinations (36).

In the present study, we confirmed our previous finding that perceived Gestalt stimuli do not elicit the early occipital stimulus-locked oscillation in SZ. Herrmann and Mecklinger (37) have demonstrated that the early occipital oscillation is modulated by the similarity of the current stimulus to the target stimulus and have proposed that this oscillation reflects a template-matching process. Thus, for the NC in this study, the elicitation of the early occipital oscillation by Square stimuli may reflect the status of these stimuli as targets. The task instructions to “press one button if you see a square, otherwise press the other button” gave priority to responding to the Square stimuli, which is corroborated by the RT patterns. The absence of the early occipital oscillation for SZ may indicate a failure to engage this process.

We have proposed that measures of neural synchrony are sensitive to the integrity of neural circuitry in schizophrenia (11, 12). Impaired cortical circuitry would be unable to synchronize properly, leading to the perceptual distortions and failures of cognitive integration that characterize schizophrenia. Supporting this hypothesis, postmortem brain studies have revealed abnormalities in several aspects of neuronal morphology in schizophrenia, including decreased density of inhibitory interneurons (1), and decreased somal size (38) and spine density (27–29) of pyramidal cells. Because local interneuron networks appear to be crucial for the generation of neural synchrony (6, 7), it is plausible that abnormalities in interneurons, and/or the excitatory glutamatergic input that drives them (4, 5, 39), could result in dysfunctional neural circuits. The evidence for cortical hyperexcitability in schizophrenia (34) is also consistent with decreased local circuit inhibition.

Of particular interest are the findings that the inhibitory connections that chandelier cells make onto pyramidal cells are abnormal (30). Because they provide inhibitory input to the axon initial segment of pyramidal cells, chandelier cells are in an excellent position to control the timing of pyramidal cell spikes (40). Furthermore, pyramidal cell excitability is strongly influenced by chandelier cell input (41), so decreased inhibitory output from chandelier cells could increase the excitability of pyramidal cells, while decreasing synchrony between them. Consistent with this model and the evidence for *N*-methyl-D-aspartate receptor hypofunction in schizophrenia (5), an *N*-methyl-D-aspartate antagonist has been shown to increase the

excitability of pyramidal cells while decreasing spike bursts (42), which may play a role in synchronizing cell assemblies.

Dysfunctional thalamocortical circuitry could also play a role in abnormal γ -band synchronization in schizophrenia (10). Thalamocortical loops are likely to be involved in synchronizing cortical circuits in the γ band (43, 44), because thalamocortical projections influence the membrane potential of cortical pyramidal neurons and hence their propensity for γ -band oscillations (31). There is evidence for structural abnormalities in thalamic nuclei at the macroscopic and microscopic scales in schizophrenia, as well as *N*-methyl-D-aspartate receptor abnormalities (45). In the future the possibility of correlations between high and low frequency bands should be examined, because Llinás *et al.* (46)

have proposed that such correlations are signs of abnormal thalamocortical synchrony.

In summary, these data support the hypothesis that abnormal γ -band synchrony in schizophrenia reflects neural circuit dysfunction that is related to the symptomatology of this disorder.

This work was supported by a Veterans Affairs Research Enhancement Award Program, a Veterans Affairs Merit Award, and National Institute of Mental Health Grant R01 40799 (to R.W.M.); a Veterans Affairs Merit Award (to P.G.N. and M.A.N.); and a Young Investigator Award (to K.M.S.) from the National Alliance for Research on Schizophrenia and Depression. K.M.S. is a Research Enhancement Award Program Fellow.

1. Benes, F. M. (2000) *Brain Res. Rev.* **31**, 251–269.
2. Lewis, D. A. & Gonzalez-Burgos, G. (2000) *Brain Res. Bull.* **52**, 309–317.
3. Selemon, L. D. & Goldman-Rakic, P. S. (1999) *Biol. Psychiatry* **45**, 17–25.
4. Grunze, H. C. R., Rainnie, D. G., Hasselmo, M. E., Barkai, E., Hearn, E. F., McCarley, R. W. & Greene, R. W. (1996) *J. Neurosci.* **16**, 2034–2043.
5. Olney, J. W., Newcomer, J. W. & Farber, N. B. (1999) *J. Psychiatr. Res.* **33**, 523–533.
6. McBain, C. J. & Fisahn, A. (2001) *Nat. Rev. Neurosci.* **2**, 11–23.
7. Whittington, M. A. & Traub, R. D. (2003) *Trends Neurosci.* **26**, 676–682.
8. Engel, A. K. & Singer, W. (2001) *Trends Cogn. Sci.* **5**, 16–25.
9. Tallon-Baudry, C. & Bertrand, O. (1999) *Trends Cogn. Sci.* **3**, 151–162.
10. Llinás, R. & Ribary, U. (2001) *Ann. N.Y. Acad. Sci.* **929**, 166–175.
11. Kwon, J. S., O'Donnell, B. F., Wallenstein, G. V., Greene, R. W., Hirayasu, Y., Nestor, P. G., Hasselmo, M. E., Potts, G. F., Shenton, M. E. & McCarley, R. W. (1999) *Arch. Gen. Psychiatry* **56**, 1001–1005.
12. Spencer, K. M., Nestor, P. G., Niznikiewicz, M. A., Salisbury, D. F., Shenton, M. E. & McCarley, R. W. (2003) *J. Neurosci.* **23**, 7407–7411.
13. Schall, J. D. (2003) *Curr. Opin. Neurobiol.* **13**, 182–186.
14. Silverstein, S. M., Kovács, I., Corry, R. & Valone, C. (2000) *Schizophr. Res.* **43**, 11–20.
15. Uhlhaas, P., Silverstein, S. M., Phillips, W. A. & Lovell, P. G. (2004) *Schizophr. Res.* **68**, 249–260.
16. Rodriguez, E., George, N., Lachaux, J.-P., Martinerie, J., Renault, B. & Varela, F. J. (1999) *Nature* **397**, 430–433.
17. American Psychiatric Association (1994) *Diagnostic and Statistical Manual of Mental Disorders* (Am. Psychiatric Assoc., Washington, DC), 4th Ed.
18. Kay, S. R., Fiszbein, A. & Opler, L. A. (1987) *Schizophr. Bull.* **13**, 261–276.
19. Makeig, S., Bell, A. J., Jung, T.-P. & Sejnowski, T. J. (1996) *Adv. Neural Inf. Process. Syst.* **8**, 145–151.
20. Keselman, H. J. & Rogan, J. C. (1980) *Psychophysiology* **17**, 499–503.
21. Woelburn, T., Eckhorn, R., Frien, A. & Bauer, R. (2002) *NeuroReport* **13**, 1881–1886.
22. Andreasen, N. C. (1983) *The Scale for the Assessment of Negative Symptoms (SANS)* (Univ. of Iowa, Iowa City).
23. Andreasen, N. C. (1984) *The Scale for the Assessment of Positive Symptoms (SAPS)* (Univ. of Iowa, Iowa City).
24. Phillips, W. A. & Silverstein, S. M. (2003) *Behav. Brain Sci.* **26**, 65–138.
25. Kopell, N., Ermentrout, G. B., Whittington, M. A. & Traub, R. D. (2000) *Proc. Natl. Acad. Sci. USA* **97**, 1867–1872.
26. Davis, K. L., Stewart, D. G., Friedman, J. I., Buchsbaum, M., Harvey, P. D., Hof, P. R., Buxbaum, J. & Haroutunian, V. (2003) *Arch. Gen. Psychiatry* **60**, 443–456.
27. Broadbelt, K., Byne, W. & Jones, L. B. (2002) *Schizophr. Res.* **58**, 75–81.
28. Garey, L. J., Ong, W. Y., Patel, T. S., Kanani, M., Davis, A., Mortimer, A. M., Barnes, T. R. E. & Hirsch, S. R. (1998) *J. Neurol. Neurosurg. Psychiatry* **65**, 446–453.
29. Glantz, L. A. & Lewis, D. A. (2000) *Arch. Gen. Psychiatry* **57**, 65–73.
30. Volk, D. W., Pierri, J. N., Fritschy, J.-M., Auh, S., Sampson, A. R. & Lewis, D. A. (2002) *Cereb. Cortex* **12**, 1063–1070.
31. Steriade, M., Amzica, F. & Contreras, D. (1996) *J. Neurosci.* **16**, 392–417.
32. Eichhammer, P., Wiegand, R., Kharraz, A., Languth, B., Binder, H. & Hajak, G. (2004) *Schizophr. Res.* **67**, 253–259.
33. Hoffman, R. E., Hawkins, K. A., Gueorguieva, R., Boutros, N. N., Rachid, F., Carroll, K. & Krystal, J. H. (2003) *Arch. Gen. Psychiatry* **60**, 49–56.
34. Hoffman, R. E. & Cavus, I. (2002) *Am. J. Psychiatry* **159**, 1093–1102.
35. ffytche, D. H., Howard, R. J., Brammer, M. J., David, A., Woodruff, P. & Williams, S. (1998) *Nat. Neurosci.* **1**, 738–742.
36. Hubl, D., Koenig, T., Strik, W., Federspiel, A., Kreis, R., Boesch, C., Maier, S. E., Schroth, G., Lovblad, K. & Dierks, T. (2004) *Arch. Gen. Psychiatry* **61**, 658–668.
37. Herrmann, C. S. & Mecklinger, A. (2001) *Vis. Cogn.* **8**, 593–608.
38. Pierri, J. N., Volk, C. L. E., Auh, S., Sampson, A. & Lewis, D. A. (2001) *Biol. Psychiatry* **58**, 466–473.
39. Woo, T.-U. W., Walsh, J. P. & Benes, F. M. (2004) *Arch. Gen. Psychiatry* **61**, 649–657.
40. Klausberger, T., Magill, P. J., Márton, L., Roberts, J. D. B., Cobden, P. M., Buzsáki, G. & Somogyi, P. (2003) *Nature* **421**, 844–848.
41. Zhu, Y., Stornetta, R. L. & Zhu, J. J. (2004) *J. Neurosci.* **24**, 5101–5108.
42. Jackson, M. E., Homayoun, H. & Moghaddam, B. (2004) *Proc. Natl. Acad. Sci. USA* **101**, 8467–8472.
43. Jones, E. G. (2001) *Trends Neurosci.* **24**, 595–601.
44. Llinás, R. R., Leznik, E. & Urbano, F. J. (2002) *Proc. Natl. Acad. Sci. USA* **99**, 449–454.
45. Clinton, S. M. & Meador-Woodruff, J. H. (2004) *Schizophr. Res.* **69**, 237–253.
46. Llinás, R. R., Ribary, U., Jeanmonod, D., Kronberg, E. & Mitra, P. P. (1999) *Proc. Natl. Acad. Sci. USA* **96**, 15222–15227.